Supporting Information

In-modified Sn-MOFs with high catalytic performance in formate electrosynthesis from aqueous carbon dioxide

Jiaying Yan[a], Xuanyu Wang[a], Fanghua Ning[a], Jin Yi[a], Yuyu Liu[a,*], Kai Wu[b,*]

[a] Institute for Sustainable Energy, College of Sciences, Shanghai University, Baoshan District, Shanghai 200444, China.

[b] Nanotechnology Research Institute, College of Materials and Textile Engineering, Jiaxing University, Jiaxing 314001, China.

---

*E-mail addresses: liuyuyu2014@126.com (Y. Liu); wk220802@zjxu.edu.cn (K. Wu).

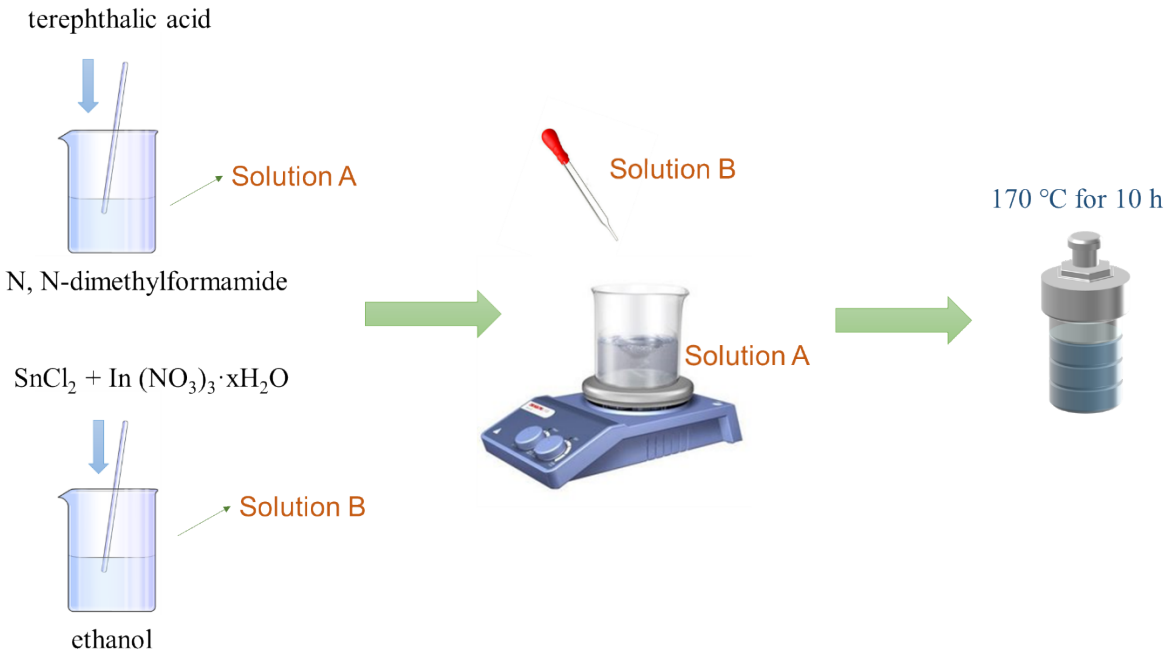

Fig. S1. Schematic illustration of the material synthesis process.

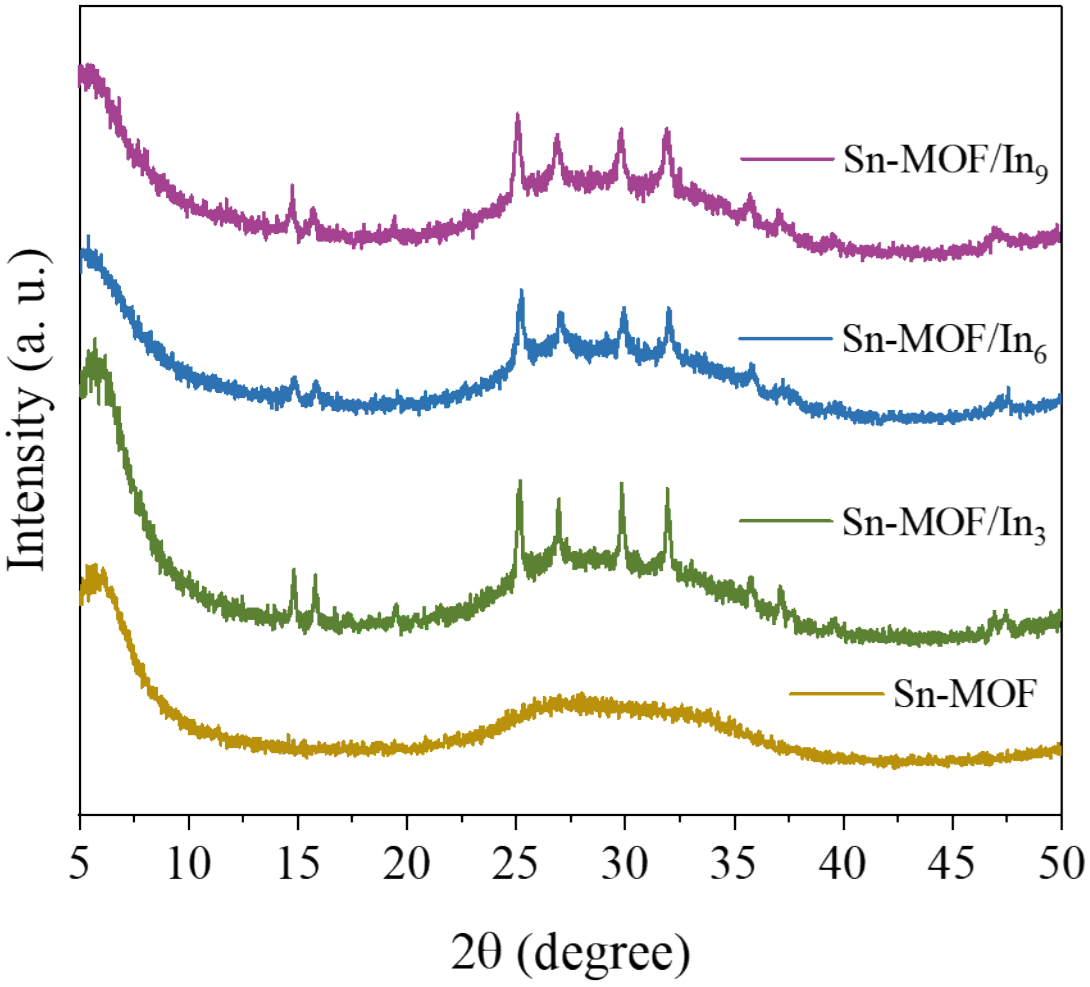

Fig. S2. XRD patterns of Sn-MOF, Sn-MOF/In_3, Sn-MOF/In_6, Sn-MOF/In_9.

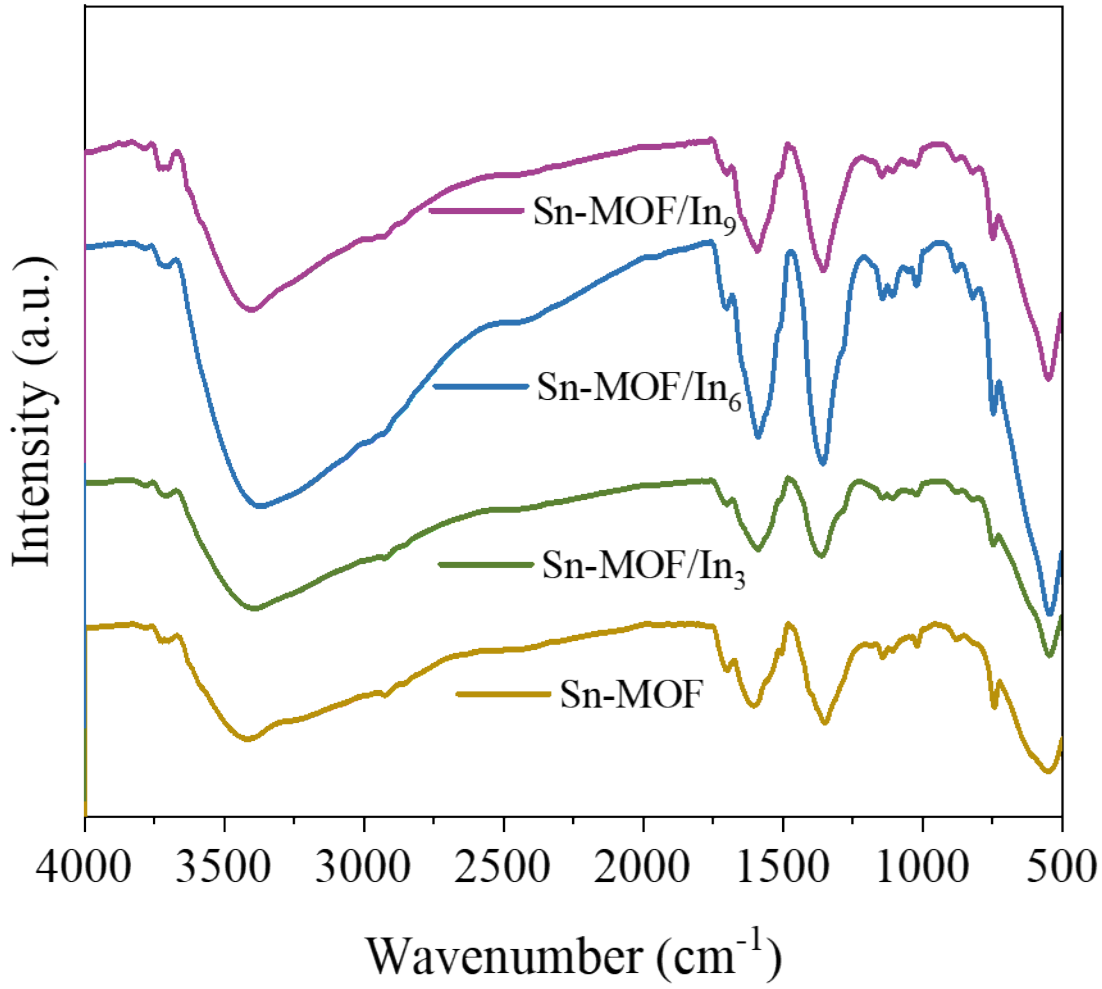

Fig. S3. FTIR patterns of Sn-MOF, Sn-MOF/In_3, Sn-MOF/In_6, Sn-MOF/In_9.

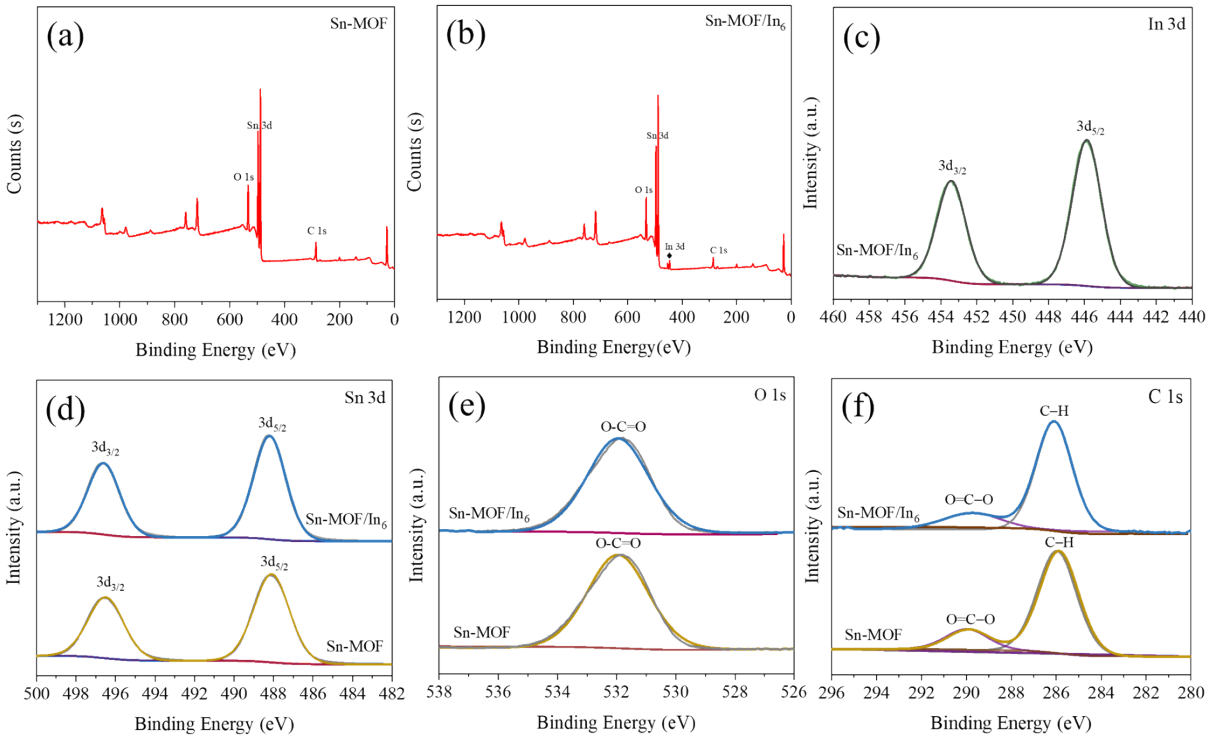

Fig. S4. XPS full spectrum of (a) Sn-MOF, (b) Sn-MOF/In_6. The corresponding high resolution XPS spectra of the (c) In 3d, (d) Sn 3d, (e) O 1s and (f) C 1s spectra of Sn-MOF and Sn-MOF/In_6.

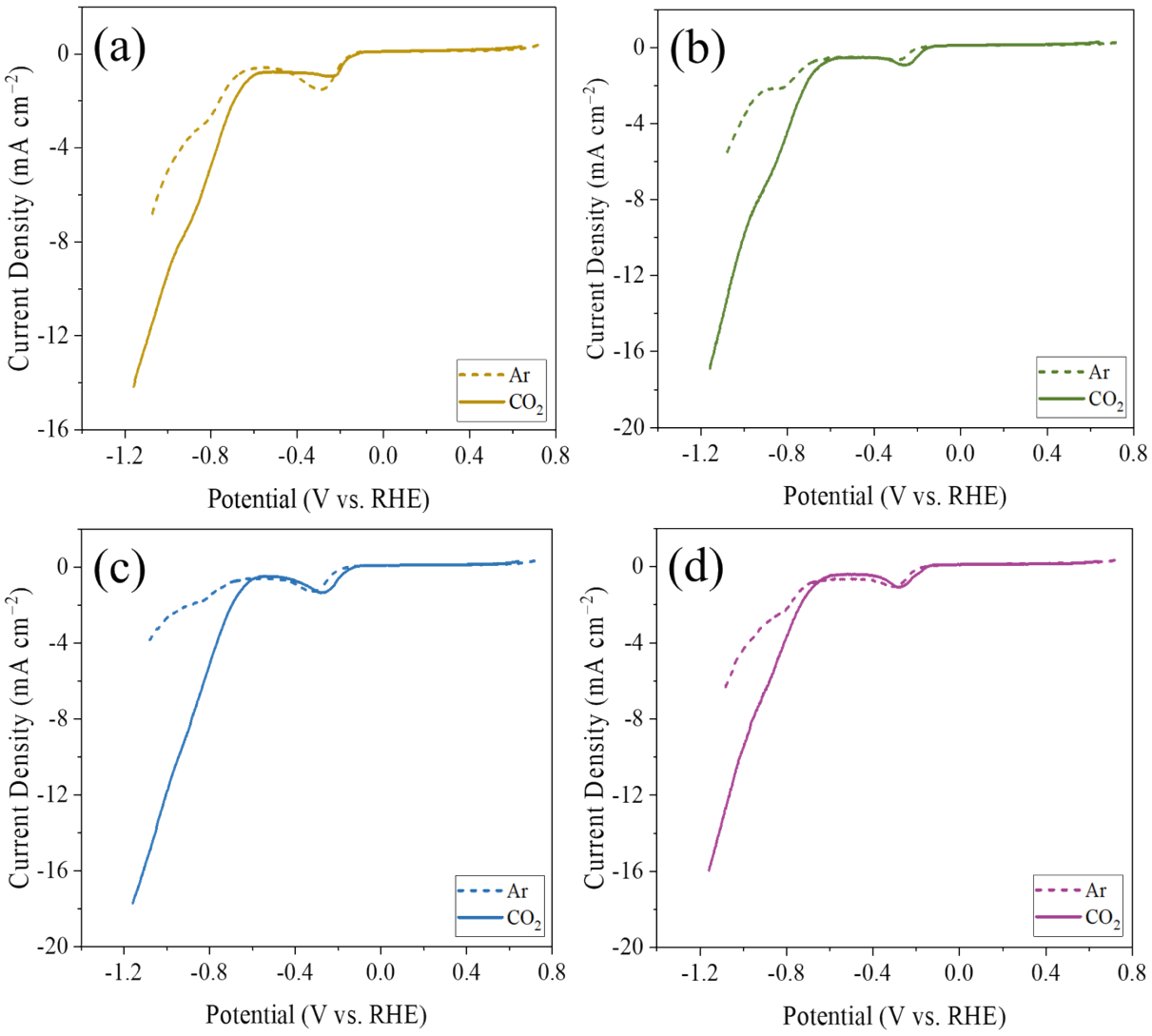

Fig. S5. LSV curves of (a) Sn-MOF (b) Sn-MOF/In_3 (c) Sn-MOF/In_6 (d) Sn-MOF/ In_9.

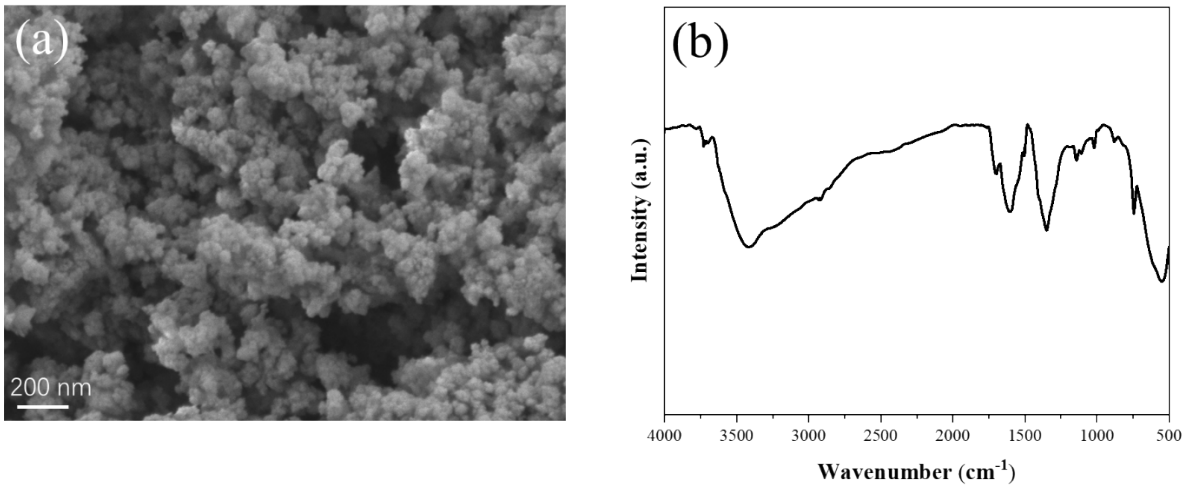

Fig. S6. (a) SEM image (b) FTIR pattern of Sn-MOF/In_6 after stability test.

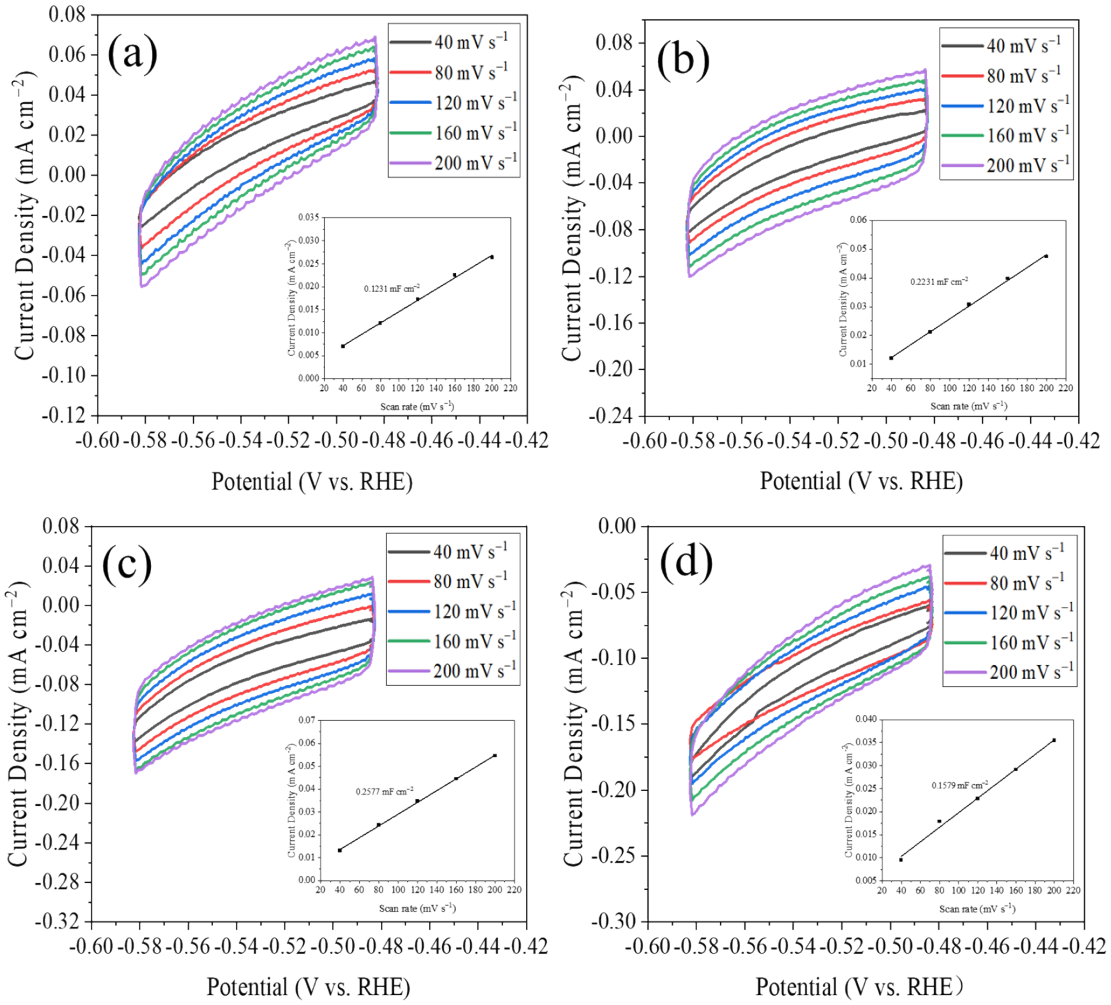

Fig. S7. CV curves of the catalysts at different sweep speeds: (a) Sn-MOF; (b) Sn-MOF/In_3, (c) Sn-MOF/In_6, (d)Sn-MOF/In_9 (The embedded graph is Double-layer capacitance against scan rates of each catalyst material).

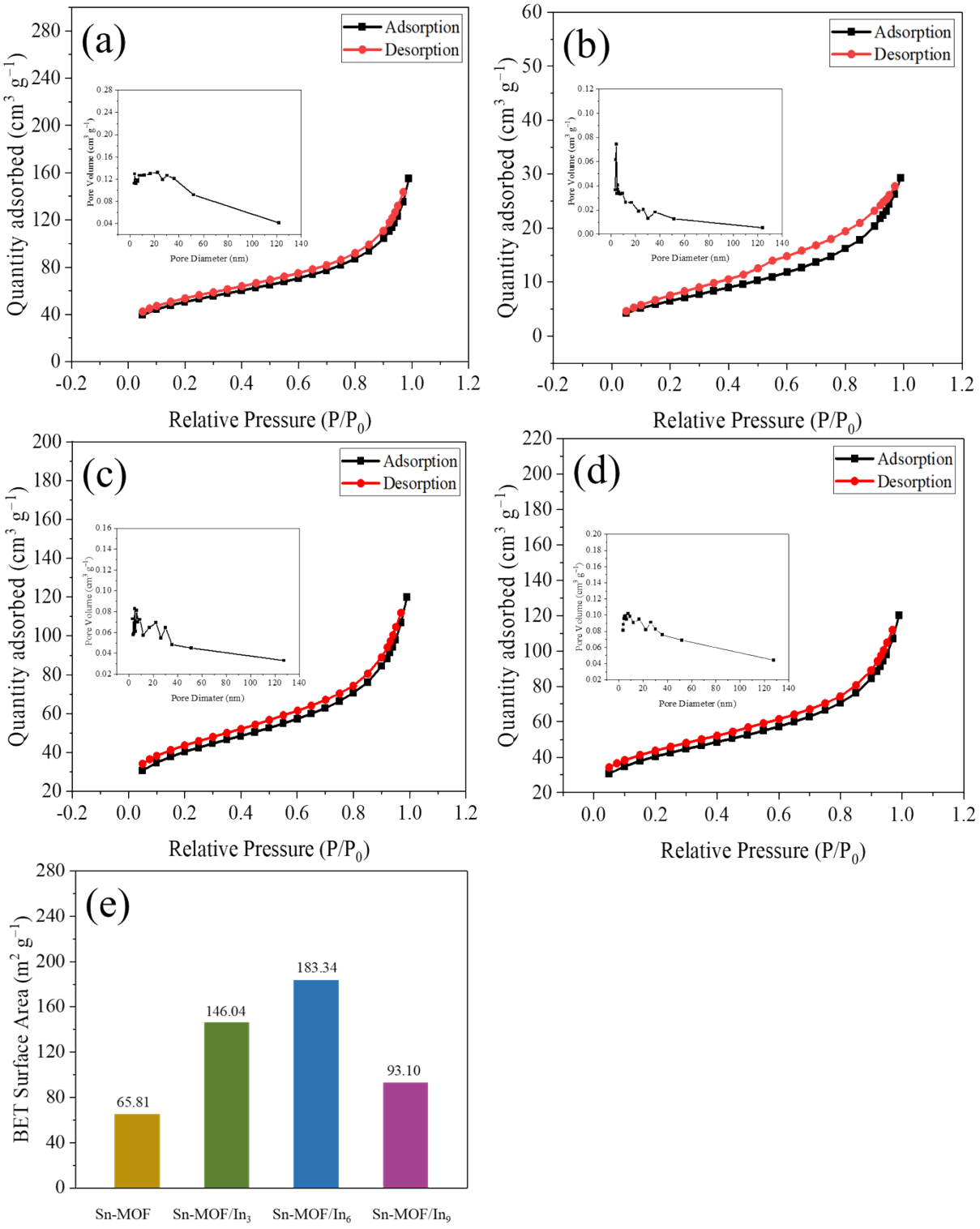

Fig. S8. The nitrogen adsorption-desorption isotherms of (a) Sn-MOF (b) Sn-MOF/In$_3$ (c) Sn-MOF/In$_6$ (d) Sn-MOF/In$_9$ (The embedded graph is the pore size distribution curves of each catalyst material). (e) BET surface area of the four catalysts.

Table S1. Inductively Coupled Plasma Optical Emission Spectrometer (ICP-OES) results for Indium contents in the serious of catalysts.

Material	Sn-MOF	Sn-MOF/In_3	Sn-MOF/In_6	Sn-MOF/In_9
In (wt %)	0 %	1.75 %	3.16 %	4.54 %

Table S2. The conclusion of Sn/In bimetallic catalysts in CO_2ER.

Materials	$FE_{formate}$	Potential	Electrolyte	Ref.
Indium Tin Oxide Nanocrystals	87%	−0.85 V_{RHE}	1.0 M KOH	[1]
In–Sn alloy catalysts $In_{0.90}Sn_{0.10}$	92%	−1.2 V_{RHE}	0.1 M $KHCO_3$	[2]
In-Sn alloy core-shell nanoparticles	86%	−0.9 V_{RHE}	0.1 M $KHCO_3$	[3]
In-O-ultrathin-SnS_2 nanosheets	88.6%	−1.2 V_{RHE}	0.5 M $KHCO_3$	[4]
Sn-MOF/In_6	97.5%	−0.96 V_{RHE}	0.5 M $KHCO_3$	This work

Table S3. BET specific surface area and pore volume aperture data

Material	Specific surface area ($m^2\ g^{-1}$)	Pore diameter (nm)	Pore volume ($cc\ g^{-1}$)
Sn-MOF	65.18	3.85	0.068
Sn-MOF/In_3	146.04	3.62	0.133
Sn-MOF/In_6	183.34	3.61	0.175
Sn-MOF/In_9	93.101	3.41	0.096

Table S4. The conclusion of BET specific surface area of Sn-MOF materials applied in various application field.

Material	BET specific surface area	Application field	Ref.
Sn-MOF	48.679 $m^2 g^{-1}$	its adsorption application for Acid Red 3R	5
Facile synthesis of Sn(II)-MOF using waste PET bottles	292 $m^2 g^{-1}$	Role of surface charge reversal in adsorption of toxic ions	6
Sn(II)-BDC MOF	17 $m^2 g^{-1}$	Preferential and efficient adsorption of anionic dyes	7
Fe_3O_4@Sn-MOF	59.949 $m^2 g^{-1}$	photocatalytic performance	8
Sn-MOF (as precursors)	72.76 $m^2 g^{-1}$	superior lithium and sodium storage	9
Sn-MOF (for synthesis Sn-MOF@CNT nanocomposite)	309 $m^2 g^{-1}$	detection of hydrogen peroxide	10
Sn-MOF (for synthesis hexahedron SnS_2/C)	30.1915 $m^2 g^{-1}$	lithium-ion batteries	11
Sn-MOF/In_6	183.3 $m^2 g^{-1}$	Electrochemical reduction of CO_2	This work

Reference

1. H. R. Jhong, U. O. Nwabara, S. Shubert-Zuleta, N. S. Grundish, B. Tandon, L. C. Reimnitz, C. M. Staller, G. K. Ong, C. A. S. Cabezas, J. B. Goodenough, P. J. A. Kenis and D. J. Milliron, *Chem. Mat.*, 2021, **33**, 7675-7685.
2. Q. Lai, N. Yang and G. Q. Yuan, *Electrochem. Commun.*, 2017, **83**, 24-27.
3. J. G. Wang, S. L. Ning, M. Luo, D. Xiang, W. Chen, X. W. Kang, Z. Jiang and S. W. Chen, *Appl. Catal. B-Environ.*, 2021, **288**, 119979.
4. X. X. Zhang, M. Y. Jiao, Z. P. Chen, X. Ma, Z. H. Wang, N. L. Wang, X. P. Zhang and L. C. Liu, *Chem. Eng. J.*, 2022, **429**.
5. D. Li, L. L. Huang, Y. Tian, T. T. Liu, L. Zhen and Y. J. Feng, *Appl. Catal. B-Environ.*, 2021, **292**, 120119.
6. A. Ghosh and G. Das, *J. Environ. Chem. Eng.*, 2021, **9**, 105288.
7. A. Ghosh and G. Das, *Microporous Mesoporous Mat.*, 2020, **297**, 110039.
8. L. Yue, Y. Cao, Y. Han, Z. Li, X. Luo and Y. Liu, *J. Alloy. Compd.*, 2021, **870**, 159339.
9. X. C. Li, C. J. He, J. Zheng, W. K. Ye, W. H. Yin, B. H. J. Tang and Y. C. Rui, *J. Alloy. Compd.*, 2020, **842**, 155605.
10. S. Rani, B. Sharma, R. Malhotra, S. Kumar, R. S. Varma and N. Dilbaghi, *Environ. Res.*, 2020, **191**, 110005.
11. X. Y. Xiao, F. J. Zhao, J. Liu, Z. Wang, Q. X. Sui and M. X. Tan, *Mater Lett*, 2021, **296**, 129877.